Natural Convection Past Inclined Porous Layers

N. Rudraiah

V. Wilfred

UGC-DSA Centre in Fluid Mechanics,
Department of Mathematics,
Central College
Bangalore University,
Bangalore 560001, India

This paper describes a study of combined Rayleigh-Bénard convection and Tollmien-Schlichting type of instability of a fluid in an inclined layer bounded by two permeable beds. Several types of flows, depending on the value of the Prandtl number, Pr, are studied using a fast convergent power series technique. Two different convective movements, longitudinal and transverse rolls, based on different Prandtl numbers, are reported. The effect of slip at the nominal surface is to augment the instability and change the critical Grashof number, Gr, and critical Rayleigh number, Ra, markedly for small permeability parameter σ, being independent of Gr and Ra for large σ. The effect of inclination ϕ is to inhibit the onset of instability in the case of air and to augment it in the case of mercury. It is shown that at maximum inclination (i.e., $\phi = \pi/2$), the instability sets in as transverse rolls, irrespective of the value of Pr. In the case of mercury, the transverse rolls exist for all ϕ, whereas in the case of air, they are limited only to certain ϕ. The cell pattern changes dramatically in the range $\phi = \pi/6$–$\pi/4$.

1 Introduction

The instability of an inclined layer of fluid bounded on both sides by permeable beds, due to combined thermal stratification and viscous shear is investigated in this paper because of its natural occurrence and its importance in the process of technology (for example, chemical engineering and some oil recovery techniques). It is also of interest in many geophysical problems (for example, the determination of reservoir characteristics in the geothermal region) and biomechanical problems (for example, blood flow in pulmonary alvelor sheet, see Fung and Tang [1, 2]) where the layer is bounded on both sides by porous material. In the geothermal region, the main mechanism of transfer of heat from the deep igneous rocks to shallow depths is buoyancy induced convection. Meteoric liquid percolating down to depth in a permeable formation is heated directly or indirectly by the intruded magma and is then driven buoyantly upward to the top of the aquifer where it can be trapped through drill holes. A viable geothermal reservoir usually consists of a sloping layer bounded on both sides by porous beds. Therefore, the criterion for the onset of convection in such a model considered in this paper may shed some insight on the study of transport processes in geothermal reservoirs.

The instability of a layer of fluid due to thermal stratification (known as Rayleigh-Bernard problem, see Chandrasekhar [3]) or due to viscous shear (known as Tollmien-Schlichting type of oscillations, see Betchov and Criminal, Jr. [4]) has been extensively investigated when the layer is bounded by impermeable rigid boundaries. Much attention has also been given to the study of instability of an inclined layer of fluid bounded on both sides by rigid impermeable plates (see Hart [5], Ruth [6], and Unny [7]). Natural convection in an inclined porous layer is also given considerable attention (see Bories and Combarnous [8], Kaneko, et al. [9], and Combarnous and Aziz [10]). However, we know relatively little about the instability of an inclined layer of fluid bounded on both sides by a porous material, which is considered in this paper.

The core problem here is to specify the proper boundary conditions at the permeables boundaries, since the vertical transport of heat depends strongly on what happens near the boundaries. Until recently, it was assumed that the no-slip boundary conditions are valid at the permeable boundaries. However, Beavers and Joseph ([11], hereafter called BJ) have shown that this no-slip condition is no longer valid at the porous boundaries and postulated the slip boundary condition called the BJ slip condition and verified it experimentally. This BJ condition was later confirmed experimentally by others (Beavers et al. [12], Taylor [13], and Rajasekhara [14]). Recently Channabasappa and Ranganna [15] have established the existence of a slip even in the case of an inclined channel. This velocity slip not only causes skewing of the main flow velocity profile in the channel but also permits a nonzero, streamwise disturbance velocity at the walls. The existence of the slip at the permeable boundary is based on the assumption of laminar flow. Therefore it is of interest to determine the condition for the transition from conduction to convective flow, which is the object of this paper. Here, we study the linear stability of a laminar flow in a channel bounded on both sides by a permeable material and inclined at an angle ϕ to the horizontal (Fig. 1). The novel feature of the linear stability problem considered here is the coupling between

Contributed by the Applied Mechanics Division for publication in the JOURNAL OF APPLIED MECHANICS.

Discussion on this paper should be addressed to the Editorial Department, ASME, United Engineering Center, 345 East 47th Street, New York, N.Y. 10017, and will be accepted until two months after final publication of the paper itself in the JOURNAL OF APPLIED MECHANICS. Manuscript received by ASME Applied Mechanics Division, April 1981; final revision, Spetember 1981.

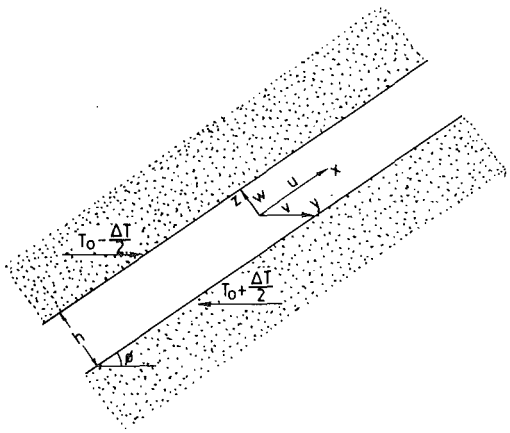

Fig. 1 Physical model

Rayleigh-Bénard type of instability due to uniform heating from below and cooling from above and Tollmien-Schlichting wave-like instability due to shear.

When the channel is horizontal and bounded on one side by a permeable bed, Sparrow, et al. [16] have investigated the linear stability using finite-difference technique. We note that the difficulty and the computer time required in solving the stability equation using finite difference technique has precluded a detailed study of the present problem. Hence the solution technique used in the present study is the classical power series method (Sparrow, et al. [17], and Ruth [6]) which is found to be a fast converging method. It is shown that the instability sets in at a lower Grashof number than that of the fluid in the channel bounded on both sides by rigid impermeable boundaries due to reduction in friction at the bounding surfaces. In particular, it is shown that there exists a fairly close analogy between convective motions in the present problem and in a fluid layer bounded by rigid boundaries.

2 Mathematical Formulation

The physical configuration of the problem under study is shown in Fig. 1. The fluid is contained between two parallel, porous layers of infinite extent, separated by a distance "h" apart and inclined at an angle ϕ to the horizontal. The temperature difference between the layers is ΔT, the upper layer having temperature $T_0 - \Delta T/2$ and the lower $T_0 + \Delta T/2$. Cartesian coordinate system (x, y, z) is taken as shown in Fig. 1, with corresponding velocity components (u, v, w).

For this configuration, the governing equations of motion for a Boussinesq fluid, made dimensionless using h for length scale, ν/h for velocity scale, ΔT for temperature, and $\rho g h$ for pressure, are

$$\nabla \cdot \mathbf{q} = 0 \tag{2a}$$

$$\frac{\partial \mathbf{q}}{\partial t} + (\mathbf{q}\cdot\nabla)\mathbf{q} = -\eta\nabla p + \eta\mathbf{a} - \mathrm{Gr}(T - T_0)\mathbf{a} + \nabla^2\mathbf{q} \tag{2b}$$

$$\frac{\partial T}{\partial t} + (\mathbf{q}\cdot\nabla)\mathrm{T} = \frac{1}{\mathrm{Pr}}\nabla^2 T \tag{2c}$$

where $\mathbf{q}$ is the velocity, T the temperature, T_0 the ambient temperature, p the pressure, ρ the density, $\mathbf{a} = -(\sin\phi, 0, \cos\phi)$, the gravity vector,

$\eta = gh^3/\nu^2$

$\mathrm{Gr} = \eta\beta\Delta T$, the Grashof number,

$\mathrm{Pr} = \dfrac{Cp\mu}{K}$ the Prandtl number

g the gravitational acceleration, μ the viscosity, ν the kinematic viscosity, β the thermal expansion coefficient, C_p the constant pressure specific heat and K is the thermal conductivity. Equations (2a)-(2c) reduce to those given by Hart [5] when $\phi = 90\text{-}\delta$ and with suitable dimensionless parameters.

The boundary conditions are,

$$\frac{du}{dz} = -\alpha\sigma(u_{B1} - Q_1) \text{ at } z = \frac{1}{2} \tag{2d}$$

$$\frac{du}{dz} = \alpha\sigma(u_{B2} - Q_2) \text{ at } z = -\frac{1}{2} \tag{2e}$$

$$v = w = 0 \text{ at } z = \pm\frac{1}{2} \tag{2f}$$

$$T = T_0 \pm \frac{1}{2} \text{ at } z = \pm\frac{1}{2} \tag{2g}$$

$$p = 0 \text{ at } x = 0, z = 0 \tag{2h}$$

where u_{B1} and u_{B2} are the slip velocities at the upper and lower interfaces, respectively, and Q_1 and Q_2 are the Darcy velocities at the edge of the boundary layers, i.e., $z = \pm 1/2 \pm 1/\sigma$ (see Rudraiah and Veerbhadraiah [18] where they have shown that the boundary layer is of order $1/\sigma$).

The Darcy velocity in the bed is given by,

$$Q = -\frac{\eta}{\sigma^2}\left[\frac{\partial p}{\partial x} + \left\{1 - \frac{\mathrm{Gr}}{\eta}(T - T_0)\right\}\sin\phi\right] \tag{2i}$$

where $\sigma = h/\sqrt{k}$ is the permeability parameter, k is the permeability of the porous material, and α is the slip parameter. This Darcy velocity is valid away from the nominal surface (see Rudraiah and Masuoka [19]).

Conditions (2d) and (2e) are the BJ slip conditions and conditions (2g) imply that the boundaries are isothermal. The Darcy equation (2i) is obtained under the assumption of the same pressure and temperature in the flows above and in the bed.

2.1 Basic Flow. The flow is due to an imbalance between the pressure and buoyancy forces when $\mathrm{Gr} \neq 0$. At low Gr, this motion forms the base flow, in which the velocity u is only in the axial direction and is a function of z and inclination ϕ only. The corresponding temperature is a function of z only and pressure is a function of both x and z. Thus the required basic flow satisfying the boundary conditions (2d)-(2h) is,

$$u_b = \frac{\mathrm{Gr}\sin\phi}{6}\left[z^3 - \left(\frac{1}{4} + f\right)z\right] \tag{2j}$$

$$u_{B2} = -u_{B1} = \frac{\mathrm{Gr}\sin\phi}{12}f \tag{2k}$$

$$T_b = T_0 - z \tag{2l}$$

$$P_b = -\left(z + \frac{\mathrm{Gr}}{2}z^2\right)\cos\phi - x\sin\phi \tag{2m}$$

$$Q = -\frac{\mathrm{Gr}\sin\phi}{2}z \tag{2n}$$

$$Q_2 = -Q_1 = \frac{\mathrm{Gr}\sin\phi}{2}\left(\frac{1}{2} + \frac{1}{\sigma}\right) \tag{2o}$$

$$f = \frac{\sigma + 6\alpha}{\sigma(2 + \alpha\sigma)}\left[1 + \frac{12\alpha}{\sigma(6\alpha + \sigma)}\right] \tag{2p}$$

where the sufffix b denotes the base flow.

2.2 The Perturbation Equations. At sufficiently large Gr, the conduction base flow regime, discussed in Section 2.1, becomes unstable and suffers a transition to convection regime. Transitions resulting in transverse rolls with their axes in the y-direction are considered in this paper. For this, we

Table 1 Critical a, Gr, and Ra for Pr = 0.025 and 0.71.

Pr	σ	ϕ = 10 deg			ϕ = 30 deg		
		a_c	$(\mathrm{Gr})_c$	$(\mathrm{Ra})_c$	a_c	$(\mathrm{Gr})_c$	$(\mathrm{Ra})_c$
0.025	∞	2.889	31100.413	777.5103	2.773	13661.636	341.5409
	10,000	2.883	30869.604	771.7401	2.767	13555.529	338.8882
	2000	2.861	29988.052	749.7013	2.744	113149.011	328.7253
	1000	2.833	28973.359	724.3340	2.715	12679.048	316.9762
	250	2.663	24460.890	611.5223	2.542	10581.099	264.5473
	100	2.373	20016.291	501.5323	2.237	8551.1534	213.7788
0.71	∞	3.095	2527.4172	1794.4662	2.822	5596.4447	3973.4757
	10,000	3.087	2511.0511	1782.8462	2.816	5521.6223	3920.3518
	2000	3.073	2449.1400	1738.8894	2.793	5248.7324	3726.60
	1000	3.050	2378.9218	1689.0344	2.766	4958.8829	3520.8068
	250	2.943	2072.4968	1471.4727	2.622	3925.1275	2786.8405
	100	2.787	1749.1672	1241.9087	2.388	3181.1417	2258.6109
		ϕ = 50 deg			ϕ = 90 deg		
0.025	∞	2.783	9449.1286	236.2282	2.702	7657.120	191.428
	10,000	2.732	9374.8320	234.3708	2.695	7596.1617	189.9040
	2000	2.709	9089.9037	227.2476	2.674	7362.1555	184.0539
	1000	2.681	8760.0795	219.002	2.646	7090.8989	177.2725
	250	2.508	7286.0908	182.1523	2.471	5877.2908	146.9323
	100	2.201	5866.5191	146.663	2.164	4713.9528	117.8488
0.71	∞	2.868	7644.4398	5427.5523	2.810	8037.5955	5706.6928
	10,000	2.860	7599.8691	5381.7070	2.803	7973.2631	5661.0168
	2000	2.833	7334.8705	5207.7580	2.780	7726.7036	5485.9595
	1000	2.80	7056.1279	5009.8508	2.749	7441.6597	5283.5783
	250	2.601	5861.8610	4161.9231	2.557	6176.4118	4385.2523
	100	2.267	4777.4387	3391.9814	2.219	4981.0913	3536.5748

superimpose on the flow a small symmetrical disturbance of the form

$$u = u_b(z) + u'(x, y, z, t)$$
$$v = v'(x, z, t),\ w = w'(x, z, t)$$
$$T = T_b(z) + T'(x, z, t) \tag{2q}$$
$$p = p_b(x, z) + p'(x, z, t)$$

where the primes denote the perturbed quantities which are assumed to be very small compared to the base flow. Substituting (2q) into the equations (2a) - (2c), linearizing and assuming that all the perturbed quantities vary in the form

$$(\text{function of } z)\ \mathrm{Exp}\,(iax + ct) \tag{2r}$$

we get,

$$(D^2 - a^2 - c)(D^2 - a^2)W - a^2 \mathrm{Gr}\cos\phi\,\Theta - ia\,\mathrm{Gr}\sin\phi D\Theta + (ia^3 u_b + ia\,D^2 u_b)W - iau_b D^2\,W = 0 \tag{2s}$$

and

$$(D^2 - a^2 - \mathrm{Pr}\,c)\,\Theta + \mathrm{Pr}\,W - \mathrm{Pr}\,iau_b\Theta = 0 \tag{2t}$$

where W is the velocity, Θ the temperature, $c(= cr + ici)$ the wave velocity, a the horizontal wave number, and $D = d/dz$. The corresponding boundary conditions are,

$$\Theta = W = DW \pm \frac{1}{\alpha\sigma} D^2 W = 0 \text{ at } z = \pm\frac{1}{2} \tag{2u}$$

We note that when $u_B = 0$ (i.e., quiescent state) and $\phi = 0$ equations (2s) and (2t) tend to the usual Rayleigh-Benard equations given by Chandrasekhar [3].

3 Marginal Stability Analysis

Since there are no external constraints like magnetic field, rotation, or salinity gradient on the motion, we assume that the marginal state is valid immediately after transition so that $c = 0$ in equations (2s) and (2t).

We shall consider the cases:

(*i*) Pr = 0 (Pure Tollmien-Schlichting instability)
(*ii*) Pro, $\phi = 0$ (Rayleigh-Benard Problem)
(*iii*) Pr $\neq$ 0 (combined Rayleigh Bénard and Tollmien-Schlichting instability)

3.1 The Case When Pr = 0. In this case shear would be dominant and it corresponds to thermally perfectly conducting fluids. Then equation (2t) becomes,

$$(D^2 - a^2)\Theta = 0 \tag{3a}$$

The solution of this equation satisfying the condition (2a) is $\Theta = 0$.

That is, the temperature perturbation vanishes and the instability is strictly due to shearing. In this case, equation (2s) using equation (2j), takes the form

$$(D^2 - a^2)^2 W + \left[\frac{ia^3 \mathrm{Gr}'}{6}\left\{z^3 - \left(\frac{1}{4} + f\right)z\right\} + iaGr'\,z\right]W - \frac{ia\mathrm{Gr}'}{6}\left\{z^3 - \left(\frac{1}{4} + f\right)z\right\}D^2 W = 0 \tag{3b}$$

where $\mathrm{Gr}' = \mathrm{Gr}\sin\phi$.

We note that, since Gr scales with $\sin\phi$, a solution for one particular angle will provide stability condition for all angles. A solution of equation (3b) is obtained in Section 4 using the power series method.

3.2 The case when $\phi = 0$. This is the usual Rayleigh-Bénard problem with porous boundaries. In this case equations (2s) and (2t) take the form,

$$(D^2 - a^2)^2 W - a^2 \mathrm{Gr}\,\Theta = 0 \tag{3c}$$

and

$$(D^2 - a^2)\Theta + \mathrm{Pr}\,W = 0 \tag{3d}$$

These simplify to the form

$$(D^2 - a^2)^3 W + a^2 \mathrm{Ra}\,W = 0 \tag{3e}$$

where Ra = Pr•Gr, is the Rayleigh number and Pr does not appear explicitly. The eigenvalues of equation (3e) are determined using the power series method as explained in Section 4.

3.3 The Case When Pr $\neq$ 0. Here we have the coupling between Tollmien-Schlichting wave-like instability due to shear and Rayleigh-Bénard type of instability due to uniform heating from below and cooling from above. Equations (2s) and (2t) using equation (2j) take the form,

$$(D^2 - a^2)^2 W - a^2 \mathrm{Gr}\cos\phi\,\Theta - ia\,\mathrm{Gr}\sin\phi\,D\Theta + \left[\frac{1}{6}ia^3 \mathrm{Gr}\sin\phi\left\{z^3 - \left(\frac{1}{4} + f\right)z\right\} + ia\,\mathrm{Gr}\sin\phi z\right]W - \frac{1}{6}ia\,\mathrm{Gr}\sin\phi\left\{z^3 - \left(\frac{1}{4} + f\right)z\right\}D^2 W = 0 \tag{3f}$$

and

$$(D^2-a^2)\Theta+\Pr W-\frac{1}{6}ia\Pr \mathrm{Gr}\sin\phi\left\{z^3-\left(\frac{1}{4}+f\right)z\right\}\Theta=0 \tag{3g}$$

4 The Power Series Solution

In this section, the power series solution for equations (3*f*) and (3*g*) are obtained for Pr $\neq$ 0. The solutions for Pr = 0 and ϕ = 0 can be obtained as particular cases.

A general solution of equations (3*f*) and (3*g*) can be constructed in the form

$$W(z)=\sum_{k=1}^{\infty}b_k z^{k-1} \tag{4a}$$

$$\Theta(z)=\sum_{k=1}^{\infty}c_k z^{k-1} \tag{4b}$$

where b_k and c_k are arbitrary constants. These constants are determined by substituting equations (4*a*) and (4*b*) into equations (3*f*) and (3*g*).

Assuming,

$$b_k=Sb_{kn}G_n,\ c_k=Sc_{kn}G_n \tag{4c}$$

where

$$G_n=(b_1,b_2,b_3,b_4,c_1,c_2) \tag{4d}$$

is the general solution vector Sb_{kn} and Sc_{kn} are particular solution vectors, we obtain

$$Sb_{kn}=(\delta_{k1},\delta_{k2},\delta_{k3},\delta_{k4},0,0)\ \text{for}\ 1\le k\le 4$$

$$Sc_{kn}=(0,0,0,0,\delta_{k1},\delta_{k2})\ \text{for}\ 1\le k\le 2$$

where δ_{ki} is the Kronecker delta.

For $k > 4$,

$$\begin{aligned}Sb_{kn}=\frac{1}{(k-1)(k-2)(k-3)(k-4)}\Big[&2a^2(k-3)(k-4)Sb_{k-2,n}\\&-a^4Sb_{k-4,n}+a^2\mathrm{Gr}\cos\phi Sc_{k-4,n}\Delta_{1,k-4}\\&+ia\,\mathrm{Gr}\sin\phi(k-4)Sc_{k-3,n}\Delta_{1,k-3}\\&-\mathrm{Gr}\sin\phi\Big\{\frac{1}{6}ia^3Sb_{k-7,n}\Delta_{1,k-7}-\Big(\frac{1}{6}ia^3\Big(\frac{1}{4}+f\Big)\\&-ia+\frac{1}{6}ia(k-6)(k-7)\Big)Sb_{k-5,n}\Delta_{1,k-5}\\&+\frac{1}{6}ia\Big(\frac{1}{4}+f\Big)(k-4)(k-5)Sb_{k-3,n}\Big\}\Big]\end{aligned} \tag{4e}$$

and for $k > 2$,

$$\begin{aligned}Sc_{kn}=\frac{1}{(k-1)(k-2)}\Big[&a^2Sc_{k-2,n}-\Pr Sb_{k-2,n}\\&+\frac{1}{6}ia\Pr\mathrm{Gr}\sin\phi Sc_{k-5,n}\Delta_{1,k-5}\\&-\frac{1}{6}ia\Pr\mathrm{Gr}\sin\phi\Big(\frac{1}{4}+f\Big)Sc_{k-3,n}\Delta_{1,k-3}\Big]\end{aligned} \tag{4f}$$

where

$$\Delta_{nm}=0,\ m<n$$

$$\Delta_{nm}=1,\ m\ge n$$

Since G_n is arbitrary and nonzero when the solution is nontrivial, it has been removed from the preceding equations. The constants b_i (i = 1 – 4) and c_j (j = 1, 2) must be chosen to satisfy the boundary conditions (2*u*). The condition for the nontrivial solution of these constants leads to the characteristic equation,

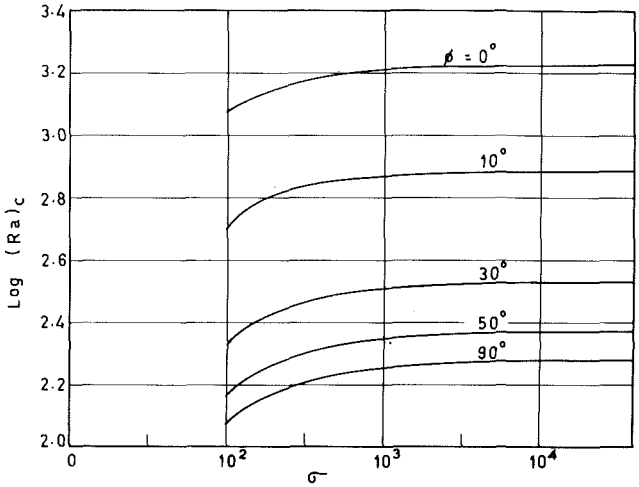

Fig. 2 Effect of σ on $(Ra)_c$ for Pr = 0.025

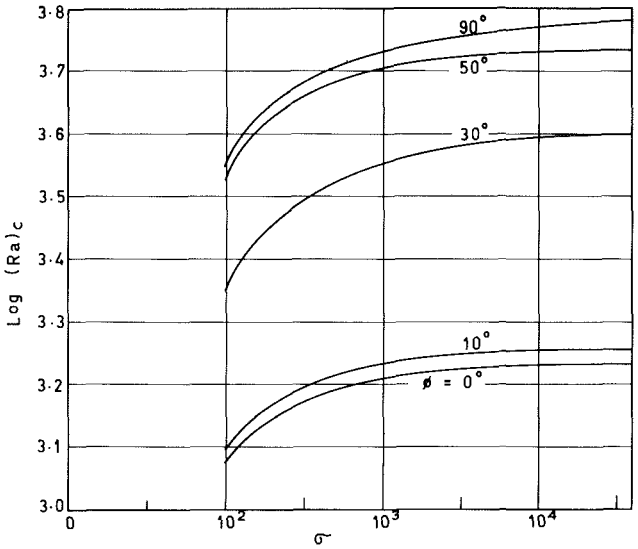

Fig. 3 Effect of σ on $(Ra)_c$ for Pr = 0.71

$$|A_{mn}|=0 \tag{4g}$$

where

$$\begin{aligned}A_{1n}&=Sb_{kn}(0.5)^{k-1}\\A_{2n}&=Sb_{kn}(-0.5)^{k-1}\\A_{3n}&=Sb_{kn}\Big[(k-1)(0.5)^{k-2}+\frac{1}{\alpha\sigma}(k-1)(k-2)(0.5)^{k-3}\Big]\\A_{4n}&=Sb_{kn}\Big[(k-1)(-0.5)^{k-2}\\&\quad-\frac{1}{\alpha\sigma}(k-1)(k-2)(-0.5)^{k-3}\Big]\\A_{5n}&=Sc_{kn}(0.5)^{k-1}\\A_{6n}&=Sc_{kn}(-0.5)^{k-1}\end{aligned} \tag{4h}$$

where k ranges from 1–∞.

The required eigenvalues are determined using the following numerical procedure. For a particular value of a, Gr is given a guess value and $|A_{mn}|$ is calculated. Using an appropriate iteration technique Gr is varied until $|A_{mn}| = 0$ up to a certain approximation. To find the critical value of Gr, its value is calculated for a range of values of a. The minimum value of Gr is taken as Gr_c and the corresponding a, a_c.

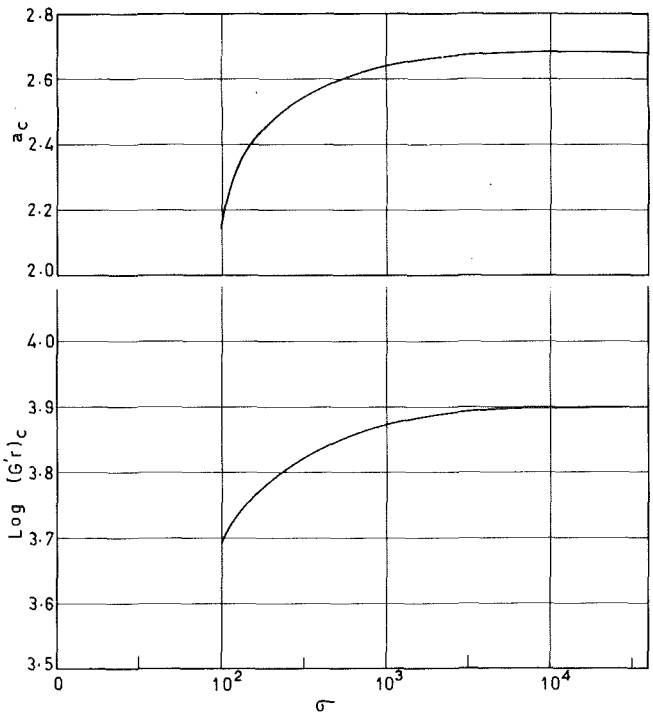

Fig. 4 Effect on σ on $(G'r)_c$ and a_c for Pr = 0

The same procedure is adopted to find the eigenvalues in the particular cases for Pr = 0 and $\phi = 0$ and the results are discussed in the following section.

5 Discussions

The stability of flow in an inclined channel bounded on both sides by porous layers with uniform heating from below and cooling from above has been studied for various inclinations ϕ, when Pr = 0 (absence of buoyancy force, i.e., pure shear), 0.025 (mercury), and 0.71 (air), for different values of σ, using a simple, fast convergent power series technique. Gr is iterated on using Newton-Raphson method up to an accuracy of 10^{-8}. The accuracy of the results depends on the number of terms used in the power series. It has been found that convergence in Gr to 8 figures accuracy requires 70 terms.

5.1 The Case When Pr $\neq$ 0. In Table 1, we have the critical Rayleigh numbers $(Ra)_c$ and critical wave numbers, a_c, for different inclinations ϕ and various values of σ when Pr = 0.025 and 0.71, with shear dominating in the former case and thermal gradient predominant in the latter case. The critical Rayleigh numbers are plotted against different σ's in Figs. 2 and 3. We note that there is a considerable decrease in $(Ra)_c$ for values of σ between 100 and 400 due to the slip at the bed, with no appreciable change for large values of σ. For large values of σ the $(Ra)_c$ tends to the values of fluid layer bounded by impermeable boundaries considered by Ruth [6]. It is interesting to note that with increase in ϕ $(Ra)_c$ decreases for Pr = 0.025 and increases for Pr = 0.71. This is because of different nature of buoyancy force phenomena in mercury and air. In the case of mercury (small Pr = 0.025) the control of convection is due to the tangential component of buoyancy which decreases with a decrease in inclination from the vertical. Hence convection sets in at a higher critical Rayleigh number as evident from Fig. 2. In the case of air, however, the normal component of buoyancy force is dominating and a very different kind of flow drive arises. This sets up a secondary flow in addition to the base flow. Hence the system becomes more unstable and a reverse phenomena to that in mercury occurs (see Fig. 3).

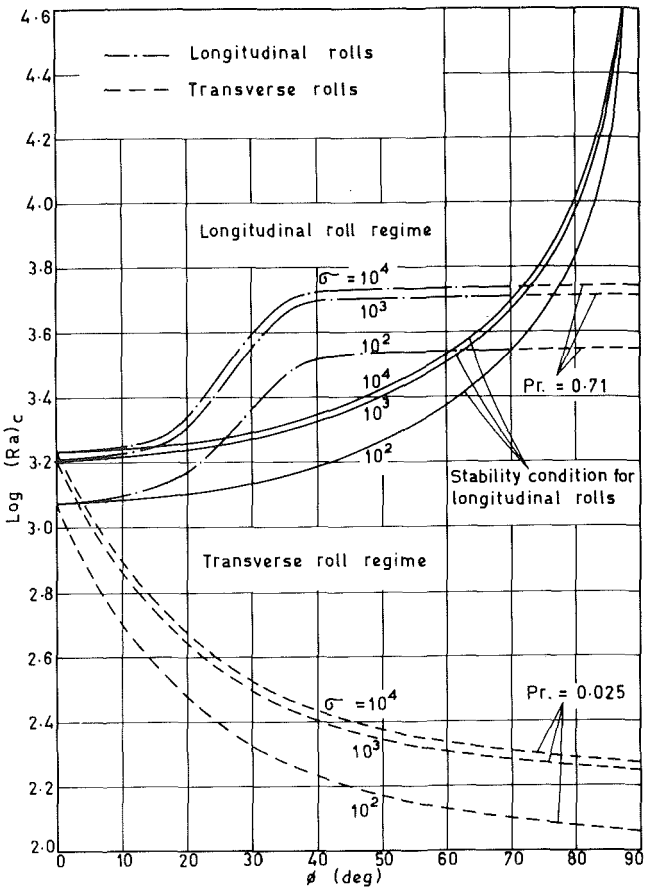

Fig. 5 Critical Ra for $\sigma = 10^2, 10^3$ and 10^4

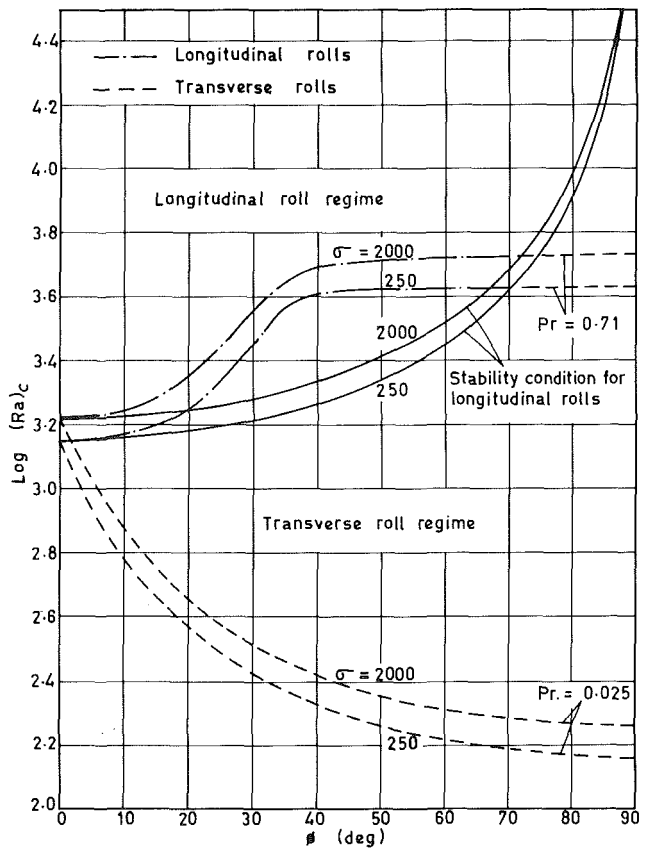

Fig. 6 Critical Ra for $\sigma = 250, 2 \times 10^3$

Table 2 Critical a and Gr ($=$ Gr sin ϕ) for Pr $=$ 0

σ	a_c	$(\acute{G}r)_c$
∞	2.688	7930.055
10,000	2.682	7867.1273
2000	2.661	7625.4095
1000	2.633	7345.0095
250	2.456	6090.8115
100	2.145	4900.4230

Table 3 Critical a, Gr, and Ra, $\phi = 0$

σ	a_c	$(Gr)_c$	$(Ra)_{c0}$
∞	3.117	2405.2982	1707.7617
10,000	3.112	2390.0779	1696.9553
2000	3.095	2332.4242	1656.0211
1000	3.076	2266.8695	1609.4773
250	2.971	1978.7683	1404.9254
100	2.824	1670.5023	1186.0566

5.2 The Case When Pr = 0. As Gr scales with sin ϕ in this case, $(\acute{G}r)_c$ the critical $\acute{G}r(=Gr \sin \phi)$ for various values of σ have been calculated and are given along with the critical wave numbers in Table 2. These provide the stability conditions for all angles.

For examples:

$$(i) \text{ for } \sigma \to \infty, (Gr)_c = \frac{7930.055}{\sin \phi} \tag{5a}$$

$$(ii) \text{ for } \sigma = 10^4, (Gr)_c = \frac{7867.1273}{\sin \phi} \tag{5b}$$

and

$$(iii) \text{ for } \sigma = 10^2, (Gr)_c = \frac{4900.4230}{\sin \phi} \tag{5c}$$

Figure 4 shows the variation of $(\acute{G}r)_c$ and a_c with respect to σ. As in Section 5.1, we note that $(Gr)_c$ decreases considerably for small values of σ and tends to a constant value for large σ because of the existence of the slip. From equations (5*a*)-(5*c*), it is clear that $(Gr)_c$ is minimum for $\phi = 90$ deg and these equations are not valid for $\phi = 0$. The case $\phi = 0$ is treated separately in the following section.

5.3 The Case When $\phi = 0$. The critical Rayleigh numbers and critical wave numbers, in this case, are computed and are shown in Table 3. The critical Rayleigh numbers are denoted as (Ra)co. Following Birikh, et al. [20], stability condition for longitudinal rolls is derived in the form

$$(Ra)_c = \frac{(Ra)_{c0}}{\cos \phi} \tag{5d}$$

where $(Ra)_{c0} = (Ra)$ when $\phi = 0$.

Transverse rolls will occur only if their $(Ra)_c$ is less than the $(Ra)_c$ in equation (5*d*). Figures 5 and 6 show the regimes where transverse and longitudinal rolls occur for various Pr and σ. For $\phi = 90$ deg, the instability results in transverse rolls irrespective of Pr. For Pr $= 0.025$, the transverse rolls occur for all inclinations. For Pr $= 0.71$, the regions where the transverse rolls occur are limited. The physical explanation for the existance of longitudinal rolls for most angles (≤ 70 deg) in the case of Pr $= 0.71$ (air) and for the existence of transverse rolls for all angles in the case of Pr $=$ 0.025 (mercury) is the same as the different nature of components of buoyancy force phenomena explained in Section 5.1. It is interesting to note that although the effect of porous boundaries is to lower the critical Rayleigh numbers, the inclinations for transverse rolls to occur are almost unaffected by σ when Pr $= 0.71$.

5.4 The Critical Wave Number, a_c. It is found that, in general, $(Gr)_c$ had to be calculated to 8 figure accuracy in order to find a_c to 4 figure accuracy. The effect of Pr and σ on

Table 4 Comparison of critical Gr for Pr $= 0.71$

ϕ	Hart [5] $(Gr)_c$ ($\sigma \to \infty$)	Ruth [6] $(Gr)_c$ ($\sigma \to \infty$)	Present case $(Gr)_c$ ($\sigma = 10^5$)
0°	2363	2405.2983	2390.0779
10°	2420	2527.4172	2511.0511
30°	6793	5596.4447	5521.6223
50°	7059	7644.4398	7579.8691
90°	8230	8037.5955	7973.2631

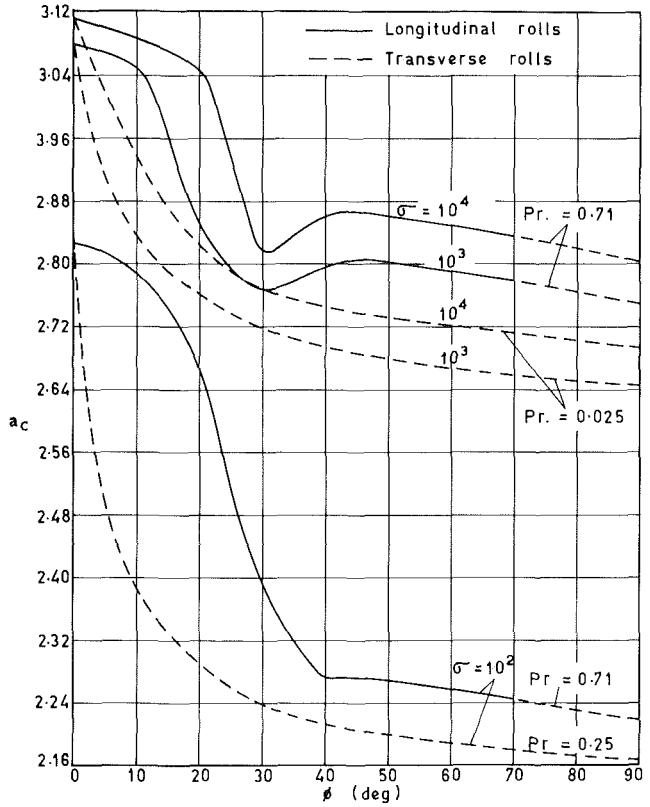

Fig. 7 Critical a for $\sigma = 10^2, 10^3$ and 10^4

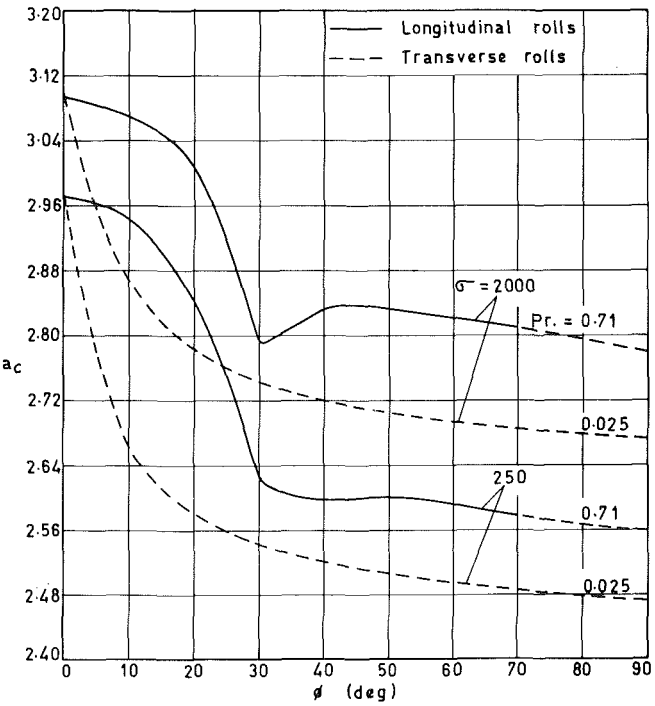

Fig. 8 Critical a for $\sigma = 250, 2 \times 10^3$

the critical wave number a_c for various inclinations are shown in Figs. 7 and 8. As σ decreases a_c also decreases. We see that in Fig. 7, the difference in a_c for $\sigma = 10^2$ and $\sigma = 10^3$ is quite large. So, as σ decreases, the wave lengths are increased. Thus, for smaller values of σ, the convection cells are elongated. Also, there is a notable change in a_c between $\phi = 30$ and $\phi = 40$ for Pr = 0.71, $\sigma = 100,250$. For these values of σ, a_c decreases in this region whereas for higher values of σ, a_c increases between $\phi = 30$ deg and $\phi = 40$ deg. We note that at Pr = 0.025, the shear would be very important and the indirect convective instability exhibiting transverse rolls with low wave numbers prevail. At Pr = 0.71 instability results in the form of longitudinals rolls having larger wave numbers.

Comparison of the results for $\sigma \to \infty$ with those for other values of σ reported in Tables 1-3 reveals that the effect of decrease in σ is to make the system less stable because of the reduction in friction at the boundaries. It is also of interest to compare our results with those of Hart [5] and Ruth [6] for $\sigma \to \infty$. This is done in Table 4 for Pr = 0.71. In this table, we have not reported the results of Unny [7] since they do not agree well with our results. Although agreement with Unny [7] is not obtained, the good agreement with Hart [5] and Ruth [6] can be interpreted as validation of the power series method employed in this paper.

6 Conclusion

The power series method employed in this paper to study convection in an inclined channel bounded on both sides by porous beds reveals a close analogy between the results of the present problem and those of a fluid layer studied by Hart [5] and Ruth [6]. Two main conclusions are as follows:

(*i*) The convective movements in the case of mercury (Pr = 0.025) are in the form of transverse rolls for all angles. In the case of air (Pr = 0.71), however, the convective movements are in the form of longitudinal rolls for the range of inclination 0 deg $\leq \phi \leq$ 70 deg and transverse rolls exist only in the narrow region of 70 deg $< \phi \leq$ 90 deg. The physical explanation for the existence of these different convective movements is given based on the dominant role of the components of buoyancy force.

(*ii*) The effect of porous boundaries is to make the system less stable due to the existence of the slip at the nominal surfaces. Further, the critical Grashof, Rayleigh, and wave numbers vary considerably with the porous parameter σ, decreasing with decreasing σ because of the reduction in friction at the porous boundaries. In the case of air, two different behaviors of critical numbers a_c are observed (Figs. 7 and 8). For 30 deg $< \phi <$ 40 deg, and for $\sigma = 100,250$, a_c decreases in this region and the convection cells are elongated. For higher values of σ, however, a_c increases for 30 deg $< \phi <$ 40 deg.

Acknowledgment

This work was sponsored by the U.G.C., India, under the DSA programme.

References

1 Fung, Y. C., and Tang, H. T., "Solute Distribution in the Flow in a Channel Bounded by Porous Layers," ASME JOURNAL OF APPLIED MECHANICS, Vol. 42, Series E, No. 3, 1975, pp. 531-535.

2 Fung, Y. C., and Tang, H. T., "Longitudinal Dispersion of Tracer Particles In the Blood Flowing in a Pulmonary Alveolar Sheet," ASME JOURNAL OF APPLIED MECHANICS, Vol. 42, Series E, No. 3, 1975, pp. 536-540.

3 Chandrasekhar, S., "Hydrodynamic and Hyrdomagnetic Stability," Claredon Press, Oxford, 1961.

4 Betchov, R., and Criminal, W. O., Jr., "Stability of Parallel Flows," Academic Press, New York, 1967.

5 Hart, J. E., "Stability of Flow in a Differently Heated Inclined Box," *Journal of Fluid Mechanics,* Vol. 47, 1971, pp. 547-576.

6 Ruth, D. W., "The Stability Criteria Governing the Transition From the Base Flow-Conduction Regime to the Transverse Roll Regime," Department of Mechanical Engineering, University of Calgary, Report 129, 1978.

7 Unny, T. E., "Thermal Instability in Differentially Heated Inclined Fluid Layers," ASME JOURNAL OF APPLIED MECHANICS, Vol. 39, 1972, pp. 41-46.

8 Bories, S. A., and Combarnous, M., "Natural Convection in a Sloping Porous Layer," *Journal of Fluid Mechanics*, Vol. 57, 1973, pp. 63-79.

9 Kaneko T., Mohtadi, M. F., and Aziz, K., "An Experimental Study of Natural Convection in an Inclined Porous Media," *International Journal of Heat and Mass Transfer*, Vol. 17, 1974, pp. 485-496.

10 Combarnous, M., and Aziz, K., "Influence of Natural Convection in Oil and Gas Reservoirs," Revnue, Institute Fr. Petrole, Vol. 25, 1970, pp. 1335-1353.

11 Beavers, G. S., and Joseph, D. D., "Boundary Conditions at a Naturally Permeable Wall," *Journal of Fluid Mechanics*, Vol. 30, 1967, pp. 197-207.

12 Beavers, G. S., Sparrow, E. M., and Magnuson, R. A., "Experiments on Coupled Parallel Flows in a Channel and a Bounding Porous Medium," ASME *Journal of Basic Engineering*, Vol. 92, Series D, 1970, pp. 845-848.

13 Taylor, G. I., "A Model for the Boundary Condition of a Porous Material," Part 1, *Journal of Fluid Mechanics*, Vol. 49, 1971, pp. 319-326.

14 Rajasekhara, B. M., 1974, Ph.D. Thesis, Bangalore University, India.

15 Channabasappa, M. N., and Ranganna, G., "Transition from Laminar Flow to Turbulence," Private Communication, 1980.

16 Sparrow, E. M., Beavers, G. S., Chen, T. S., and Lloyd, J. R., "Breakdown of the Laminar Flow Regime in Permeable Walled Ducts," ASME JOURNAL OF APPLIED MECHANICS, Vol. 40, Series E, 1973, pp. 337-342.

17 Sparrow, E. M., Golstein, R. J., and Johsson, V . K., "Thermal Instability in a Horizontal Fluid Layer: Effect of Boundary Conditions and Nonlinear Temperature Profile," *Journal of Fluid Mechanics*, Vol. 18, Part 4, 1964, pp. 513-528.

18 Rudraiah, N., and Veerabhadraiah, R., "Buoyancy Effect on the Couette Flow Past a Permeable Bed," *Journal of Mathematical and Physical Sciences*, Vol. 13, No. 6, 1979, pp. 523-539.

19 Rudraiah, N., and Masuoka, T., "Asymptotic Analysis of Natural Convection Through Horizontal Porous Layers," *International Journal of Engineering Sciences*, 1981, (accepted for publication).

20 Birikh, R. V., Gershuni, G. Z., Zhukovitskii, E. M., and Rudakov, R. N., "Hydrodynamic and Thermal Instability of a Steady Convective Flow," *Prikl, Mat. i Mekh.*, Vol. 32, No. 2, pp. 256-263.